In vivo role of neutrophil extracellular traps in antiphospholipid antibody-mediated venous thrombosis

He Meng, MD, PhD,[1] Srilakshmi Yalavarthi, MS,[1] Yogendra Kanthi, MD,[2,3] Levi F. Mazza,[1] Megan A. Elfline, MS,[4] Catherine E. Luke, LVT,[4] David J. Pinsky, MD,[2] Peter K. Henke, MD,[4] and Jason S. Knight, MD, PhD[1]

Divisions of [1]Rheumatology and [2]Cardiovascular Medicine, Department of Internal Medicine, University of Michigan Medical School; [3]Division of Cardiology, Ann Arbor Veterans Administration Healthcare System; and [4]Department of Vascular Surgery, University of Michigan Medical School, Ann Arbor, Michigan, USA

Correspondence
Jason S. Knight, M.D., Ph.D.
5520A MSRB1, 1150 W Medical Center Drive, SPC 5680
Ann Arbor, MI 48109-5680
Tel: 734-936-3257
jsknight@umich.edu

Short title: In vivo role of NETs in APS

Words (text): 4,414

Words (abstract): 224

References: 48

Tables: 0

Figures: 6

Supplementary Figures: 7

The authors have no competing interests or conflicts to disclose.

This is the author manuscript accepted for publication and has undergone full peer review but has not been through the copyediting, typesetting, pagination and proofreading process, which may lead to differences between this version and the Version record. Please cite this article as doi:10.1002/art.39938.

ABSTRACT

Objective: Antiphospholipid syndrome (APS) is a leading acquired cause of thrombotic events. While antiphospholipid antibodies have been shown to promote thrombosis in mice, the role of neutrophils has not been explicitly studied. Here, we characterized neutrophils in the context of a new model of antiphospholipid antibody-mediated venous thrombosis.

Methods: Mice were administered IgG fractions prepared from patients with APS. At the same time, flow through the inferior vena cava was reduced by a standard stenosis. Resulting thrombi were characterized for size and neutrophil content. Circulating factors and the vessel wall were also assessed.

Results: As measured by both thrombus weight and thrombosis frequency, mice treated with IgG from patients with APS demonstrated exaggerated thrombosis as compared with controls. APS thrombi were enriched for citrullinated histone H3 (a marker of neutrophil extracellular traps/NETs). APS mice also demonstrated elevated levels of circulating cell-free DNA and human IgG bound to the neutrophil surface. In contrast, circulating neutrophil numbers and markers of vessel wall activation were not appreciably different between APS and control mice. Regarding therapy, treatment with either deoxyribonuclease (which dissolves NETs) or a neutrophil-depleting antibody reduced thrombosis in APS mice to the level seen in controls.

Conclusion: These data support a mechanism whereby circulating neutrophils are primed by antiphospholipid antibodies to accelerate thrombosis. This line of investigation suggests new, immunomodulatory approaches for the treatment of APS.

INTRODUCTION

Antiphospholipid syndrome (APS), with an estimated prevalence of at least 1 in 2,000, is a leading acquired cause of both thrombosis and pregnancy loss (1). About half of cases are diagnosed in the background of systemic lupus erythematosus (SLE), while the remaining represent a standalone syndrome called primary APS (2). In contrast to other prothrombotic diatheses, APS is associated with myriad other clinical complications including thrombocytopenia, skin ulcerations, nephropathy, seizure disorder, cognitive decline, and accelerated atherosclerosis (3). Importantly, these non-clotting manifestations may continue to progress despite treatment with anticoagulation, which is the current standard of care for APS management.

With the goal of identifying novel pathways that might be amenable to targeted treatments beyond anticoagulation, there have been efforts to model APS in mice (4). Numerous studies have been published with a model of femoral vein pinch injury, whereby infusion of IgG from patients with APS (APS IgG) leads to exaggerated thrombosis (5-7). Additionally, interesting work has relied on laser injury to the cremaster microcirculation (8, 9), or ferric chloride application (10), where again the presence of APS IgG accelerates the clotting phenotype. Notably, these models have relied on direct vessel wall injury, which has unclear relevance for some human events such as venous thrombosis (the most common manifestation of APS) (11).

Historically, three cell types—endothelial cells, platelets, and monocytes—have received the majority of attention as perpetuators of APS-related thrombosis (12). This important work has demonstrated that antiphospholipid antibodies bind to proteins like beta-2 glycoprotein I (β_2GPI), which associate with cell-surface phospholipids (13). This engagement leads to cell activation and upregulation of prothrombotic molecules such as tissue factor. In particular, a two-hit hypothesis has been put forth, whereby the endothelium exists in a primed state in patients with APS, while a second event, like infection, then tips the patient toward thrombosis (14, 15).

More recently, our group and others have posited a role for neutrophils in APS (16-18). This work was spurred by a new emphasis in the thrombosis literature regarding the importance of neutrophils in pathologic clotting, and especially venous thrombosis (19). Neutrophils release extracellular chromatin-based structures, coined neutrophil extracellular traps (NETs), through a process known as NETosis (20, 21). NETs consist primarily of DNA and histones that originate from the nucleus, but are also decorated with cytoplasm-derived material, such as the granule proteins neutrophil elastase and myeloperoxidase. While NETs were originally characterized for

their role in host defense against microbes (20, 21), more recent work has suggested an additional role in thrombosis. The DNA component of NETs can activate the intrinsic coagulation cascade (22, 23). Histones stimulate platelets (24), while NET-derived proteases inactivate certain anticoagulant factors (22). In some contexts, NETs may even be an important source of tissue factor (25). Our group's work with human cells has shown that IgG isolated from patients with APS, and perhaps especially anti-β_2GPI IgG, engage with neutrophils to stimulate NETosis (16). This correlates with more cell-free DNA and NETs in the circulation of patients with APS, even in the absence of acute thrombotic events (16). Another group has shown that APS NETs, when formed, may be particularly resistant to degradation by serum deoxyribonuclease (DNase) (17). Further, low-density granulocytes (LDGs), neutrophils that are prone to exaggerated NETosis, are found in increased numbers in patients with APS (18).

Here, we have developed a model of APS venous thrombosis by reducing flow through the inferior vena cava (IVC). In the literature, and also in our hands, this model results in thrombus formation in less than 50% of control mice (17, 22, 26). In contrast, we find an 80-90% rate of thrombosis when mice are administered IgG form patients with APS. We set out to characterize neutrophils in this model.

METHODS

Human subjects. Patients were recruited from Rheumatology and Hematology clinics at the University of Michigan. All patients with APS fulfilled the laboratory and clinical requirements for APS established by the Sydney classification criteria (27), while none of the patients met American College of Rheumatology (ACR) criteria for SLE (28). Healthy volunteers were recruited through a posted flyer; exclusion criteria included history of a systemic autoimmune disease, active infection, and pregnancy. Blood was collected by phlebotomist venipuncture, and serum was prepared by standard methods and stored at -80ºC until ready for use. IgG, IgM, and IgA anti-β_2GPI, as well as IgG and IgM anticardiolipin, were determined by ELISA (Inova Diagnostics). Lupus anticoagulant (LAC) was tested according to published guidelines (29).

Preparation of human IgG. IgG was purified from APS or control sera with Protein G Agarose according to the manufacturer's instructions (Pierce). Briefly, serum was diluted in IgG binding buffer and repeatedly passed through a Protein G Agarose column (at least 5 times). IgG was eluted with 0.1 M glycine and then neutralized with 1 M Tris. This was followed by overnight dialysis against PBS at 4ºC. After passing through a 0.2-micron filter, IgG purity was verified by SDS-PAGE and Coomassie staining. IgG concentrations were determined by BCA protein assay (Pierce). All IgG preparations were confirmed to be free of endotoxin contamination as determined by a chromogenic endotoxin quantification kit (Pierce).

Animal housing, surgery, and treatments. Mice were housed in a specific pathogen-free barrier facility, and fed standard chow. Male C57BL/6 mice were purchased from The Jackson Laboratory (000664), and used at approximately 10 weeks of age. Peripheral leukocyte and platelet counts were determined with an automated Hemavet 950 counter (Drew Scientific).

Male C57BL/6 wild-type mice were administered two doses (500 µg each) of either control or APS IgG by intraperitoneal injection, 48 hours apart. Just prior to the second IgG treatment, a laparotomy was performed, and a ligature was fastened around the IVC over a blunted 30-gauge needle (which served as a spacer). After removal of the spacer, the abdomen was closed, and the mouse was allowed to recover. Here, we will refer to this procedure as the "stenosis" or "flow restriction" model. Sham procedures followed the same protocol except the ligature was passed under the IVC and then removed from the mouse without fastening. Some mice were additionally treated with DNase (Pulmozyme/dornase alfa, Genentech) immediately after surgery, 50 µg by intraperitoneal injection and 10 µg by intravenous (tail vein) injection.

Other mice were treated with two doses (50 µg each) of anti-Ly6G antibody (BioXCell, *InVivo*Plus anti m Ly-6G); these doses were administered 72 and 24 hours before the laparotomy/stenosis. Mice were humanely euthanized and thrombus formation was assessed 6 and 48 hours after laparotomy.

In addition to the stenosis model, we also performed a procedure that we here refer to as the "stasis" model. This was done essentially as described (30). Briefly, mice underwent complete ligation of the IVC and all visible contributing vessels below the renal veins. This produces full stasis. The stasis model is well characterized and consistently produces a thrombus (>97% of the time) (30). The stasis model differs from the stenosis model in that *(i)* the IVC is fully ligated and *(ii)* all visible side and back branches are also ligated.

Venous ultrasound following IVC stenosis. Anesthetized mice underwent laparotomy, and IVCs were sonographically analyzed *in vivo* by B-mode and color Doppler with a Vevo2100 40-MHz transducer and software (VisualSonics) as previously described (31).

Neutrophil purification and NETosis assay. Bone marrow neutrophils were isolated as previously described (32). Briefly, total bone marrow cells were spun on a discontinuous Percoll gradient (52%-69%-78%) at 1500xg for 30 minutes. Cells from the 69%-78% interface were collected. These cells were >95% Ly-6G-positive by flow cytometry, and had typical nuclear morphology by microscopy. To assess *in vitro* NETosis, a protocol similar to what we have described previously was employed (33). IgG stimulation was for 4 hours at 37ºC in RPMI media supplemented with 2% bovine serum albumin and 10 mM HEPES buffer. Stimulation with phorbol-12-myristate-13-acetate (PMA 100 nM, Sigma) was also for 4 hours. For immunofluorescence, cells were fixed with 4% paraformaldehyde (PFA). DNA was stained with Hoechst 33342 (Invitrogen), while protein staining was with rabbit polyclonal antibodies to myeloperoxidase (MPO) (Dako) or citrullinated histone H3 (Abcam), followed by FITC-conjugated anti-rabbit IgG (SouthernBiotech). Images were collected with an Olympus IX70 microscope and a CoolSNAP HQ2 monochrome camera (Photometrics) with Metamorph Premier software (Molecular Devices). NETs (decondensed extracellular DNA co-staining with one of the aforementioned protein markers) were quantified by two blinded observers, and digitally recorded to prevent multiple counts. The percentage of NETs was calculated after counting 10 400x fields per sample.

Thrombus sectioning and immunohistochemistry. At 6 and 48 hours, thrombi are easily separated from the vessel wall. Formalin-fixed thrombus sections were stained with a rabbit

polyclonal antibody against citrullinated histone H3 (Abcam), and an HRP-conjugated anti-rabbit secondary antibody (Jackson ImmunoResearch). Prior to antibody staining, epitope retrieval was achieved by boiling for 30 minutes in sodium citrate buffer. Color change was detected with DAB-Plus Substrate Kit (Invitrogen). Images were captured with a Biotek Cytation 5 fitted with Olympus 4x and 20x objectives, and, when necessary, stitched together with the associated Biotek software. Positively-stained surface area was quantified with ImageJ software.

Western blotting. After separation from the vessel wall, thrombi were prepared for SDS-PAGE by sonication in RIPA buffer (50 mM Tris pH 8.0, 200 mM NaCl, 0.5% Nonidet P-40, and a Roche protease inhibitor cocktail pellet). Lysates were then cleared by centrifugation at 14,000xg for 10 minutes at 4ºC. Supernatant protein concentrations were measured with the BCA Protein Assay Kit (Pierce) according to manufacturer's instructions. Samples were resolved by 15% SDS-PAGE under denaturing conditions, and transferred to a 0.45-micron nitrocellulose membrane. Primary antibodies were directed against citrullinated histone H3 and histone H3 (both from Abcam). Detection was with IRDye-labeled secondary antibodies (Rockland Immunochemicals). Images were captured and analyzed with an Odyssey imaging system (LI-COR Biosciences).

ELISA for soluble P-selectin. Plasma was tested with the Mouse sP-Selectin/CD62P Quantikine ELISA Kit (R&D Systems) according to manufacturer's instructions.

RNA preparation and quantitative polymerase chain reaction (PCR). At the time of tissue harvest, vessel walls were snap frozen in liquid nitrogen and stored at -80 degrees. Later, the walls were resuspended and mechanically homogenized in TriPure Isolation Reagent (Roche). RNA was prepared by the Direct-zol RNA MiniPrep kit (Zymo Research) according to manufacturer's instructions. RNA Integrity Number (RIN) was >7 for all included samples. cDNA was synthesized using MMLV RT (Invitrogen) and 200 ng of RNA using a MyCycler thermocyler (Bio-Rad). Quantitative PCR was with SYBR Green PCR Master Mix (Qiagen) according to manufacturer's instructions, and carried out using an ABI PRISM 7900HT (Applied Biosystems). Primers for mouse CXCL1, CCL2, IL-6, thrombomodulin, ICAM-1, VCAM-1, E-selectin, and P-selectin were purchased from Qiagen (QuantiTect Primer Assays, which have proprietary primer sequences). The housekeeping gene was GAPDH with primer sequences of 5'-ACCACAGTCCATGCCATCAC-3' and 5'-TCCACCACCCTGTTGCTGTA-3'.

Ct values were normalized to the housekeeping gene to determine ΔCt. ΔΔCt values were then determined by comparing each ΔCt to the average ΔCt for the sham group treated with control IgG. Data were presented as relative fold change by the formula $2^{\Delta\Delta Ct}$.

Flow cytometry. After lysing red blood cells, total leukocytes were stained with anti-Ly6G and anti-human-IgG (Biolegend). Staining was for 30 minutes at 4ºC. After washing, cells were fixed in 2% paraformaldehyde before analysis with a CyAn ADP Analyzer (Beckman Coulter). Further data analysis was done in FlowJo.

Measurement of cell-free DNA. Cell-free DNA was quantified in plasma using the Quant-iT PicoGreen dsDNA Assay Kit (Invitrogen) according to the manufacturer's instructions.

Statistical analysis. Data analysis was with GraphPad Prism software version 6. Normally-distributed data were analyzed by unpaired t test, and skewed data were assessed by Mann-Whitney test. For assessment of dichotomous variables (thrombosis frequency), the analysis was by Chi square. Statistical significance was defined as $p<0.05$.

Study approval. This study was reviewed and approved by the University of Michigan Institutional Review Board. Written informed consent was received from all participants prior to inclusion. The University's Institutional Animal Care and Use Committee (IACUC) approved all mouse protocols utilized in this study.

RESULTS

Mice administered APS IgG develop larger thrombi following IVC stenosis. As is detailed above, others have shown that administration of APS IgG creates a prothrombotic milieu in mice. When thrombosis is then triggered by a "second hit," APS mice develop thrombi more efficiently than controls. Here, we characterized two mouse models of venous thrombosis that have not been previously studied in the context of APS.

In the first model, the IVC is subjected to a reproducible, flow-restricting stenosis (Figure 1A), which leads to thrombosis in approximately 50% of control mice. This is referred to as a "flow restriction" or "stenosis" model (17, 22, 26). To test the role of APS IgG, we purified total IgG from 6 "triple positive" patients with primary APS (positive for IgG anti-cardiolipin, IgG anti-β_2GPI, and lupus anticoagulant), as well as from healthy volunteers. The healthy volunteer IgG was pooled to make "control IgG," which was used for all experiments here. Wild-type C57BL/6 mice were then administered IgG by two intraperitoneal injections (500 µg each, 48 hours apart). At the time of the second IgG injection, the aforementioned stenosis was introduced. 48 hours after stenosis, mice were euthanized and thrombus weight was assessed (Figure 1B). As compared with control mice, APS mice formed significantly larger thrombi (Figure 1C-D). Representative H&E staining demonstrates both red blood cell (RBC)-rich and RBC-poor regions within thrombi, a feature that is typical of human DVT (34), and which has been described by others in similar flow restriction models (17, 22, 26).

The second model differs from the stenosis model in that the IVC is fully ligated, along with ligation of all visible side and back branches. This is known as a "stasis" model (30). Resulting thrombi (which form >97% of the time in control mice) are significantly enriched in RBCs (30). It has also been reported that neutrophils and NETs play a relatively less important role in the stasis model as compared with *(i)* models utilizing flow restriction and *(ii)* authentic human deep vein thrombosis (19, 30). In contrast to experiments with the stenosis model (Figure 1B), administration of APS IgG did not lead to significantly larger thrombi when mice were subjected to the stasis model (Supplementary Figure 1). In summary, these data demonstrate that treatment with APS IgG leads to larger thrombi in a model of venous flow restriction, but not in a model of complete stasis. We therefore focused on the stenosis model for the following experiments.

APS thrombi are enriched in NETs. Regarding the mechanism of APS IgG-accelerated thrombosis, we next asked whether APS IgG could promote NETosis *in vitro*. We found that, as

compared with control IgG, APS IgG stimulated mouse neutrophils to undergo NETosis (Figure 2A). As would be expected, these *in vitro* NETs had detectable DNA, citrullinated histone H3 (Cit-H3), and myeloperoxidase (Figure 2B, and data not shown). Given that citrullinated histones are recognized as the best biochemical marker of NETs, we extended our staining for Cit-H3 to thrombus sections. While Cit-H3 was present in both APS and control thrombi, staining was especially widespread in APS thrombi (Figure 2C-D). When we analyzed corresponding H&E-stained sections, we found that regions rich in Cit-H3 staining were infiltrated by neutrophils as the predominant nucleated cells (Figure 2E). Further, quantification of Cit-H3 by western blotting revealed a significant enrichment of Cit-H3 in APS thrombi (Figure 2F). In summary, these data suggest that NETosis is exaggerated in the context of APS IgG treatment, both *in vitro* and *in vivo*.

Mice administered APS IgG develop thrombi by 6 hours. As we were interested in whether NETs might play a role as initiators of thrombosis in APS, we turned our attention from the 48-hour time point (Figures 1 and 2), to a 6-hour time point. Further, in these experiments, we added an additional control (sham) in which a laparotomy was performed, and the IVC was exposed, but *without* tying a stenosis-inducing ligature (Supplementary Figure 2A). As before, mice were treated with either control or APS IgG. No mouse in the sham groups developed an IVC thrombus, even with APS IgG administration. However, with stenosis, 50% of control mice and 100% of APS mice did develop thrombi at 6 hours (n=10 per group; Supplementary Figure 2B).

APS IgG binds neutrophils *in vivo*. We first asked whether the neutrophils might differ functionally between the 4 experimental conditions (control-sham, control-stenosis, APS-sham, APS-stenosis; Supplementary Figure 2A). We scored Ly6G-positive neutrophils for surface binding of human IgG. Interestingly, we found that both APS-sham and APS-stenosis mice were more likely to have human IgG bound to their neutrophils as compared with the control conditions (Figure 3A-B). As a surrogate for circulating NETs, we measured plasma cell-free DNA in the same mice. The only condition that showed a statistically-significant “spike” in cell-free DNA was APS-stenosis (Figure 3C), albeit with notable variability between individual mice at the 6-hour time point. In summary, neutrophils from APS IgG-treated mice are more likely to have human IgG on their surface than controls. Further, when these APS mice are subjected to IVC stenosis, they also demonstrate higher levels of cell-free DNA.

Control and APS mice have similar numbers of total neutrophils. At the 6-hour time point, we also quantified numbers of neutrophils and platelets in circulation (Figure 4A-B). While stenosis resulted in relative thrombocytopenia and neutrophilia as compared with the sham groups, control and APS mice did not differ in this regard. Further, when we focused on the one condition where some mice formed thrombi and some did not (control-stenosis), the presence of a thrombus did not clearly predict either thrombocytopenia or neutrophilia (Supplementary Figure 3). In summary, although APS IgG-treated mice are at greater risk of thrombosis, this risk does not seem to be explained by numbers of circulating neutrophils or platelets.

The vessel wall's response to stenosis is similar in control and APS mice. At the time of euthanasia (6 hours after sham or stenosis), we sampled a portion of the vessel wall just distal to the renal veins (in the region of the vessel where a thrombus formed in some mice). We then tested the expression of genes that may be indicative of vessel wall activation (Figure 4C-D, and Supplementary Figure 4). Some genes, including ICAM-1, VCAM-1, E-selectin, and P-selectin, were not regulated by any of the conditions (Supplementary Figure 4). However, for other genes, including CXCL-1, CCL-2, IL-6, and thrombomodulin, there were two interesting trends. First, when considering only the sham groups, there was upregulation in APS mice as compared with controls (Figure 4C-D and Supplementary Figure 4; compare the first and third conditions in each graph). Second, upon stenosis *both* APS and control mice demonstrated marked upregulation as compared with the sham groups, especially of CXCL-1 and CCL-2. Notably, APS and control mice did not differ as to the degree of this upregulation (Figure 4C-D and Supplementary Figure 4; compare the second and fourth conditions in each graph). In parallel, we asked whether levels of soluble P-selectin, sometimes used as a marker of endothelial activation, differed between the groups. When considering only the sham groups, P-selectin levels were higher in APS mice as compared with controls (Supplementary Figure 5). In contrast, upon stenosis there was no difference between APS and control mice (Supplementary Figure 5). In summary, we did find subtle evidence of vessel wall activation upon administration of APS IgG as compared with control IgG. However, this difference was overwhelmed by flow restriction (stenosis), which led to significant upregulation of genes that track with vessel wall activation.

NETs are present in APS thrombi at 6 hours. We found evidence of Cit-H3 staining in the 6-hour thrombi, focused at the periphery of the thrombus (where the thrombus was previously engaging the vessel wall) (Figure 5A-B and Supplementary Figure 6). Further, when assessed by western blotting, Cit-H3 content was significantly increased in 6-hour APS thrombi as

compared with controls (Figure 5C). In summary, by 6 hours, there is already an exaggeration of Cit-H3 content in APS thrombi. Whether these NETs are released because of neutrophil contact with the vessel wall, or whether NETs may form elsewhere and then associate with the periphery of the thrombus, remains to be determined.

Both neutrophil depletion and DNase abrogate thrombosis in APS mice. Finally, we turned our attention to potential therapeutics, testing them in control and APS mice at the 6-hour time point. Although there was a subtle trend toward efficacy, neither neutrophil depletion nor DNase significantly reduced thrombosis in control mice (Figure 6A). In contrast, APS mice demonstrated a marked reduction in thrombosis with either treatment (Figure 6B-C). To look at the interconnectedness between neutrophil depletion and DNase treatment, we tested thrombi of neutrophil-depleted mice for the presence of NETs. When APS thrombi form under baseline conditions, they are rich in both total histone H3 and Cit-H3 (Figure 5). Interestingly, we found that both markers were essentially absent from the thrombi of neutrophil-depleted mice (Figure 6D). This supports the idea that neutrophils are not just the source of NETs, but also the primary nucleated cells infiltrating thrombi at the 6-hour time point. Importantly, the degree of neutrophil depletion did not differ between the groups (Figure 6E). To summarize, we would highlight the fact that APS mice treated with either DNase or neutrophil depletion become essentially indistinguishable from control mice (Figure 6F), emphasizing the importance of NETosis in the acceleration of thrombosis by APS IgG.

DISCUSSION

Recent studies from our group and others have suggested a role for NETosis in the thrombotic complications of APS (16-18, 35, 36). Exposure of neutrophils to antiphospholipid antibodies promotes NETosis (16), and when NETs form in patients with APS, they seem to be relatively resistant to degradation (17). APS NETs promote thrombin generation, an effect that can be blocked by treatment with DNase (16). It is also notable that LDGs, a subset of neutrophils that are prone to exaggerated NETosis, have recently been identified in patients with APS, and especially in patients with high titers of IgG anti-β_2GPI (18). Without a proven strategy for identifying LDGs in mice (and actually without proof that they exist at all in mice), LDGs were not considered as part of our studies. We here sought to develop an *in vivo* model that would allow us to assess the stimulation of neutrophils by antiphospholipid antibodies in an environment that might recapitulate thrombus formation in humans.

Animal models have been an important tool in the APS field, in some instances leading to new considerations in patient care such as the use of hydroxychloroquine or complement inhibitors (7, 37). In terms of assessing venous thrombosis, these models have typically relied on explicit vessel-wall (and presumably endothelial) damage, which is not a usual part of human deep vein thrombus formation (where stagnant blood flow is a more important factor) (38). This study and the recent work of others have suggested that the IVC stenosis model employed here leads to a more subtle regulation of the vessel wall in response to disrupted flow (22).

We have shown for the first time that administration of IgG from patients with APS accelerates venous thrombosis in a flow restriction model, a phenotype that associates with *(i)* human IgG binding to the neutrophil surface, *(ii)* elevated levels of plasma cell-free DNA, and *(iii)* increased infiltration of NETs into the thrombi themselves. These findings are in contrast to the “stasis” model of venous thrombosis. Even with our most robust APS patient IgG, we were unable to demonstrate a clear phenotype with complete stasis. One might speculate that this relates to the relatively less important role of inflammatory cells (and perhaps especially neutrophils) under conditions of complete flow arrest (30). Indeed, others have argued that models that maintain flow are better mimickers of human deep vein thrombosis (19, 22).

Heterotypic *inter*-cellular interactions between primed neutrophils and activated platelets/endothelial cells have been recognized to facilitate NETosis in various systems (39-41). We speculate that antiphospholipid antibodies may prime neutrophils *in vivo*, but then a second signal (perhaps from the endothelium) is necessary for full activation to thrombo-

inflammatory NETosis (Supplementary Figure 7). This could be one reason for the sporadic nature of thrombi in patients with APS, and might also explain our immunhistochemical data in which Cit-H3 staining localizes to the vessel wall interface of early thrombi. However, as pointed out above, we do not have real-time data to prove these NETs were released at the vessel wall in situ. It is also possible that they formed elsewhere and then deposited along the activated endothelium. Further study on this front with intravital microscopy is needed.

A recent study demonstrated that DNase may protect against venous thrombosis in control mice, utilizing a model of flow restriction that is similar to ours (26). This is in contrast to our data, in which we only found a statistically-significant effect of DNase in APS mice. Our experiments did differ from the earlier studies in that we especially focused therapy on the early time point of 6 hours. It is possible that NETosis—perhaps triggered by the emerging thrombus itself—is a key regulator of thrombus propagation over time. Therefore, a therapeutic effect will only be revealed at later time points. In support of this hypothesis is that we found very little Cit-H3 in control thrombi at 6 hours. This is in contrast to the APS thrombi where it was readily detectable at this early time point (Figure 5C). It should also be pointed out that the model details (including spacer size) were not identical between our study and the earlier work (26). It is certainly possible that the particulars of stenosis and flow have an impact on the degree of vessel wall activation and thrombus NET content.

There is a clear need in the APS field for precision treatments that address underlying pathophysiology. Presently, patients are treated with long-term anticoagulation, a therapy that carries inherent risk and is not uniformly effective (3). In terms of DNase as a potential therapeutic, this has long been considered as a possibility in patients with SLE (42-44); however, it is unclear whether sufficient and durable plasma levels can be achieved with currently available preparations. As mechanisms of NETosis become better understood, it may be possible to use agents like peptidylarginine deiminase inhibitors or neutrophil elastase inhibitors to target the process of NETosis (45, 46), or possibly anti-interferon drugs to target the downstream effects of NETs (47). In summary, we suggest that neutrophils should continue to be explored as therapeutic targets in APS. There is also a need to extend these studies to models beyond venous thrombosis, including arterial thrombosis and thrombosis in the microvasculature (10, 15, 48).

ACKNOWLEDGEMENTS

JSK was supported by NIH K08AR066569 and a career development award from the Burroughs Wellcome Fund. YK was supported by NIH K08HL131993. The work was supported by the Arthritis National Research Foundation, as well as the Joshua (Jim) and Eunice Stone Foundation.

AUTHORSHIP AND CONFLICT OF INTEREST DISCLOSURES

The authors have no competing interests or conflicts to disclose. H.M., S.Y., Y.K., L.F.M., M.A.E., and C.E.L. conducted experiments and analyzed data. Y.K., D.J.P., P.K.H., and J.S.K. designed the study. All authors participated in writing the manuscript, and gave approval before submission.

REFERENCES

1. Gomez-Puerta JA, Cervera R. Diagnosis and classification of the antiphospholipid syndrome. Journal of autoimmunity. 2014;48-49:20-5.
2. Bertolaccini ML, Amengual O, Andreoli L, Atsumi T, Chighizola CB, Forastiero R, et al. 14th International Congress on Antiphospholipid Antibodies Task Force. Report on antiphospholipid syndrome laboratory diagnostics and trends. Autoimmunity reviews. 2014;13(9):917-30.
3. Abreu MM, Danowski A, Wahl DG, Amigo MC, Tektonidou M, Pacheco MS, et al. The relevance of "non-criteria" clinical manifestations of antiphospholipid syndrome: 14th International Congress on Antiphospholipid Antibodies Technical Task Force Report on Antiphospholipid Syndrome Clinical Features. Autoimmunity reviews. 2015;14(5):401-14.
4. Willis R, Harris EN, Pierangeli SS. Pathogenesis of the antiphospholipid syndrome. Seminars in thrombosis and hemostasis. 2012;38(4):305-21.
5. Pericleous C, Ruiz-Limon P, Romay-Penabad Z, Marin AC, Garza-Garcia A, Murfitt L, et al. Proof-of-concept study demonstrating the pathogenicity of affinity-purified IgG antibodies directed to domain I of beta2-glycoprotein I in a mouse model of anti-phospholipid antibody-induced thrombosis. Rheumatology. 2015;54(4):722-7.
6. Pierangeli SS, Vega-Ostertag ME, Raschi E, Liu X, Romay-Penabad Z, De Micheli V, et al. Toll-like receptor and antiphospholipid mediated thrombosis: in vivo studies. Annals of the rheumatic diseases. 2007;66(10):1327-33.
7. Pierangeli SS, Girardi G, Vega-Ostertag M, Liu X, Espinola RG, Salmon J. Requirement of activation of complement C3 and C5 for antiphospholipid antibody-mediated thrombophilia. Arthritis and rheumatism. 2005;52(7):2120-4.
8. Arad A, Proulle V, Furie RA, Furie BC, Furie B. beta(2)-Glycoprotein-1 autoantibodies from patients with antiphospholipid syndrome are sufficient to potentiate arterial thrombus formation in a mouse model. Blood. 2011;117(12):3453-9.
9. Proulle V, Furie RA, Merrill-Skoloff G, Furie BC, Furie B. Platelets are required for enhanced activation of the endothelium and fibrinogen in a mouse thrombosis model of APS. Blood. 2014;124(4):611-22.
10. Laplante P, Fuentes R, Salem D, Subang R, Gillis MA, Hachem A, et al. Antiphospholipid antibody-mediated effects in an arterial model of thrombosis are dependent on Toll-like receptor 4. Lupus. 2015.

11. Cervera R, Piette JC, Font J, Khamashta MA, Shoenfeld Y, Camps MT, et al. Antiphospholipid syndrome: clinical and immunologic manifestations and patterns of disease expression in a cohort of 1,000 patients. Arthritis and rheumatism. 2002;46(4):1019-27.
12. Ruiz-Irastorza G, Crowther M, Branch W, Khamashta MA. Antiphospholipid syndrome. Lancet. 2010;376(9751):1498-509.
13. Giannakopoulos B, Krilis SA. The pathogenesis of the antiphospholipid syndrome. The New England journal of medicine. 2013;368(11):1033-44.
14. Meroni PL, Borghi MO, Raschi E, Tedesco F. Pathogenesis of antiphospholipid syndrome: understanding the antibodies. Nature reviews Rheumatology. 2011;7(6):330-9.
15. Fischetti F, Durigutto P, Pellis V, Debeus A, Macor P, Bulla R, et al. Thrombus formation induced by antibodies to beta2-glycoprotein I is complement dependent and requires a priming factor. Blood. 2005;106(7):2340-6.
16. Yalavarthi S, Gould TJ, Rao AN, Mazza LF, Morris AE, Nunez-Alvarez C, et al. Release of Neutrophil Extracellular Traps by Neutrophils Stimulated With Antiphospholipid Antibodies: A Newly Identified Mechanism of Thrombosis in the Antiphospholipid Syndrome. Arthritis & rheumatology. 2015;67(11):2990-3003.
17. Leffler J, Stojanovich L, Shoenfeld Y, Bogdanovic G, Hesselstrand R, Blom AM. Degradation of neutrophil extracellular traps is decreased in patients with antiphospholipid syndrome. Clinical and experimental rheumatology. 2014;32(1):66-70.
18. van den Hoogen LL, Fritsch-Stork RD, van Roon JA, Radstake TR. Low-Density Granulocytes Are Increased in Antiphospholipid Syndrome and Are Associated With Anti-beta2 -Glycoprotein I Antibodies: Comment on the Article by Yalavarthi et al. Arthritis & rheumatology. 2016;68(5):1320-1.
19. Martinod K, Wagner DD. Thrombosis: tangled up in NETs. Blood. 2014;123(18):2768-76.
20. Brinkmann V, Reichard U, Goosmann C, Fauler B, Uhlemann Y, Weiss DS, et al. Neutrophil extracellular traps kill bacteria. Science. 2004;303(5663):1532-5.
21. Brinkmann V, Zychlinsky A. Neutrophil extracellular traps: is immunity the second function of chromatin? The Journal of cell biology. 2012;198(5):773-83.
22. von Bruhl ML, Stark K, Steinhart A, Chandraratne S, Konrad I, Lorenz M, et al. Monocytes, neutrophils, and platelets cooperate to initiate and propagate venous thrombosis in mice in vivo. The Journal of experimental medicine. 2012;209(4):819-35.
23. Gould TJ, Vu TT, Swystun LL, Dwivedi DJ, Mai SH, Weitz JI, et al. Neutrophil extracellular traps promote thrombin generation through platelet-dependent and platelet-

independent mechanisms. Arteriosclerosis, thrombosis, and vascular biology. 2014;34(9):1977-84.

24. Fuchs TA, Brill A, Duerschmied D, Schatzberg D, Monestier M, Myers DD, Jr., et al. Extracellular DNA traps promote thrombosis. Proceedings of the National Academy of Sciences of the United States of America. 2010;107(36):15880-5.

25. Kambas K, Mitroulis I, Apostolidou E, Girod A, Chrysanthopoulou A, Pneumatikos I, et al. Autophagy mediates the delivery of thrombogenic tissue factor to neutrophil extracellular traps in human sepsis. PloS one. 2012;7(9):e45427.

26. Brill A, Fuchs TA, Savchenko AS, Thomas GM, Martinod K, De Meyer SF, et al. Neutrophil extracellular traps promote deep vein thrombosis in mice. Journal of thrombosis and haemostasis : JTH. 2012;10(1):136-44.

27. Miyakis S, Lockshin MD, Atsumi T, Branch DW, Brey RL, Cervera R, et al. International consensus statement on an update of the classification criteria for definite antiphospholipid syndrome (APS). Journal of thrombosis and haemostasis : JTH. 2006;4(2):295-306.

28. Hochberg MC. Updating the American College of Rheumatology revised criteria for the classification of systemic lupus erythematosus. Arthritis and rheumatism. 1997;40(9):1725.

29. Pengo V, Tripodi A, Reber G, Rand JH, Ortel TL, Galli M, et al. Update of the guidelines for lupus anticoagulant detection. Subcommittee on Lupus Anticoagulant/Antiphospholipid Antibody of the Scientific and Standardisation Committee of the International Society on Thrombosis and Haemostasis. Journal of thrombosis and haemostasis : JTH. 2009;7(10):1737-40.

30. El-Sayed OM, Dewyer NA, Luke CE, Elfline M, Laser A, Hogaboam C, et al. Intact Toll-like receptor 9 signaling in neutrophils modulates normal thrombogenesis in mice. Journal of vascular surgery. 2015.

31. Kanthi Y, Hyman MC, Liao H, Baek AE, Visovatti SH, Sutton NR, et al. Flow-dependent expression of ectonucleotide tri(di)phosphohydrolase-1 and suppression of atherosclerosis. The Journal of clinical investigation. 2015;125(8):3027-36.

32. Knight JS, Zhao W, Luo W, Subramanian V, O'Dell AA, Yalavarthi S, et al. Peptidylarginine deiminase inhibition is immunomodulatory and vasculoprotective in murine lupus. The Journal of clinical investigation. 2013;123(7):2981-93.

33. Knight JS, Subramanian V, O'Dell AA, Yalavarthi S, Zhao W, Smith CK, et al. Peptidylarginine deiminase inhibition disrupts NET formation and protects against kidney, skin and vascular disease in lupus-prone MRL/lpr mice. Annals of the rheumatic diseases. 2014.

34. Sevitt S. The structure and growth of valve-pocket thrombi in femoral veins. Journal of clinical pathology. 1974;27(7):517-28.
35. Duarte JH. Connective tissue diseases: Neutrophil extracellular traps-a mechanism of thrombosis in patients with antiphospholipid syndrome? Nature reviews Rheumatology. 2015;11(8):444.
36. Rao AN, Kazzaz NM, Knight JS. Do neutrophil extracellular traps contribute to the heightened risk of thrombosis in inflammatory diseases? World journal of cardiology. 2015;7(12):829-42.
37. Edwards MH, Pierangeli S, Liu X, Barker JH, Anderson G, Harris EN. Hydroxychloroquine reverses thrombogenic properties of antiphospholipid antibodies in mice. Circulation. 1997;96(12):4380-4.
38. Esmon CT. Basic mechanisms and pathogenesis of venous thrombosis. Blood reviews. 2009;23(5):225-9.
39. Clark SR, Ma AC, Tavener SA, McDonald B, Goodarzi Z, Kelly MM, et al. Platelet TLR4 activates neutrophil extracellular traps to ensnare bacteria in septic blood. Nature medicine. 2007;13(4):463-9.
40. Caudrillier A, Kessenbrock K, Gilliss BM, Nguyen JX, Marques MB, Monestier M, et al. Platelets induce neutrophil extracellular traps in transfusion-related acute lung injury. The Journal of clinical investigation. 2012;122(7):2661-71.
41. Gupta AK, Joshi MB, Philippova M, Erne P, Hasler P, Hahn S, et al. Activated endothelial cells induce neutrophil extracellular traps and are susceptible to NETosis-mediated cell death. FEBS letters. 2010;584(14):3193-7.
42. Verthelyi D, Dybdal N, Elias KA, Klinman DM. DNAse treatment does not improve the survival of lupus prone (NZB x NZW)F1 mice. Lupus. 1998;7(4):223-30.
43. Macanovic M, Sinicropi D, Shak S, Baughman S, Thiru S, Lachmann PJ. The treatment of systemic lupus erythematosus (SLE) in NZB/W F1 hybrid mice; studies with recombinant murine DNase and with dexamethasone. Clinical and experimental immunology. 1996;106(2):243-52.
44. Davis JC, Jr., Manzi S, Yarboro C, Rairie J, McInnes I, Averthelyi D, et al. Recombinant human Dnase I (rhDNase) in patients with lupus nephritis. Lupus. 1999;8(1):68-76.
45. Martinod K, Demers M, Fuchs TA, Wong SL, Brill A, Gallant M, et al. Neutrophil histone modification by peptidylarginine deiminase 4 is critical for deep vein thrombosis in mice. Proceedings of the National Academy of Sciences of the United States of America. 2013;110(21):8674-9.

46. Cools-Lartigue J, Spicer J, McDonald B, Gowing S, Chow S, Giannias B, et al. Neutrophil extracellular traps sequester circulating tumor cells and promote metastasis. The Journal of clinical investigation. 2013.

47. Grenn RC, Yalavarthi S, Gandhi AA, Kazzaz NM, Nunez-Alvarez C, Hernandez-Ramirez D, et al. Endothelial progenitor dysfunction associates with a type I interferon signature in primary antiphospholipid syndrome. Annals of the rheumatic diseases. 2016.

48. Thalin C, Demers M, Blomgren B, Wong SL, von Arbin M, von Heijne A, et al. NETosis promotes cancer-associated arterial microthrombosis presenting as ischemic stroke with troponin elevation. Thrombosis research. 2016;139:56-64.

FIGURE LEGENDS

Figure 1 APS IgG promotes venous thrombosis. **A,** Schematic of the inferior vena cava (IVC) stenosis model, in which a ligature is fastened just distal to the renal veins to introduce a standard restriction in flow. **B,** IgG was purified from either APS patients or healthy controls and administered to mice (2 intraperitoneal injections, 48 hours apart). At the time of the second injection, the IVC was narrowed (stenosed), as described in panel A. 48 hours after stenosis, thrombus weight was measured. Each data point represents an individual mouse. Horizontal lines denote group means. APS groups were compared to the control group; *p<0.05, **p<0.01. **C,** Ultrasound imaging of the IVC at time=0 (left) or 48 hours later (for IgG-injected mice). In the Doppler images, color (either red or blue) indicates active flow. The yellow dashed lines delineate areas in which flow is excluded due to thrombosis. Images are representative of 3 mice per group. **D,** Representative thrombus sections for APS and control mice stained with H&E (4x images stiched together). For APS, the left two thrombi are from the APS 1 group and the right two from the APS 5 group. Note the mix of RBC-rich (red) and RBC-poor (pink) areas.

Figure 2 APS IgG promotes the release of NETs *in vitro* and *in vivo*. **A,** Mouse neutrophils were stimulated with PMA, control IgG, or APS IgG. NETosis was scored by immunofluorescence microscopy. N=4-6 per condition. Mean and SEM are depicted. **p<0.01, ****p<0.0001. **B,** Representative microscopy from the experiment of panel A. DNA is stained blue and citrullinated histone H3 (Cit-H3) green. NETs are identified as extracellular areas of blue and green overlap. Scale bar=50 microns. **C,** 48-hour thrombus sections (as in Figure 1) were stained by H&E, Hoechst 33342 (for DNA), and anti-Cit-H3 (for NETs). Staining is represenative of n=4 per group. The dashed yellow circle indicates an area that is viewed at higher magnification in panel E. **D,** Quantification of Cit-H3-positive surface area for panel C. Mean and SEM are depicted for n=4 per group. *p<0.05. **E,** Upon higher magnification, neutrophils are detected in regions that stain prominently for Cit-H3. Three represenative neutrophils are marked by yellow arrowheads (although essentially every cell in this field is a neutrophil). Scale bar=50 microns. **F,** Western blotting of total thrombus protein for citrullinated histone H3 (Cit-H3) and total histone H3 (H3). Quantification is in arbitrary units. For quantification, N=6 per group (for APS: 3 from the APS 1 group and 3 from the APS 5 group). Mean and SEM are depicted. **p<0.01.

Figure 3 Mice treated with APS IgG have higher levels of neutrophil-bound IgG and plasma cell-free DNA at 6 hours. Both "sham" and "stenosis" mice underwent a laparotomy with exposure of the IVC; however, only stenosis mice had the IVC narrowed. "Control" mice were treated with control IgG. "APS" mice were treated with APS 1 IgG. **A,** Nucleated cells from peripheral blood were subjected to flow cytometry. Represenative staining is shown for Ly6G (a neutrophil marker) and human IgG, after gating for neutrophils by forward- and side-scatter. **B,** Quantification of the experiment presented in panel A. **C,** Cell-free DNA was determined in plasma for the indicated groups. For panels B and C, each data point represents an individual mouse. Horizontal lines denote group means. Statistically-significant comparisons are shown; **p<0.01, ***p<0.001.

Figure 4 Mice treated with control and APS IgG do not differ for numbers of circulating cells or markers of vessel wall activation at 6 hours. Both "sham" and "stenosis" mice underwent a laparotomy with exposure of the IVC; however, only stenosis mice had the IVC narrowed. "Control" mice were treated with control IgG. "APS" mice were treated with APS 1 IgG. **A** and **B,** Neutrophil and platelet counts were determined in peripheral blood. **C** and **D,** Quantitative PCR analysis of vessel walls, obtained distal to the renal veins (in the region of the vessel where a thrombus formed in some mice). For all panels, each data point represents an individual mouse. Horizontal lines denote group means. Statistically-significant comparisons are shown; *p<0.05, **p<0.01.

Figure 5 Thrombi from APS IgG-treated mice contain NETs at 6 hours. All mice presented in this figure underwent the stenosis procedure. **A,** Thrombus sections were stained by H&E, Hoechst 33342 (DNA), and anti-citrullinated histone H3 (Cit-H3). At 6 hours, the RBC-rich areas make up the majority of the thrombi, while the RBC-poor areas are largely confined to the periphery. Red arrowheads demonstrate Cit-H3 staining, which localizes to the periphery (vessel wall interface) of the APS thrombus at the 6-hour time point. The dashed yellow circle denotes an area considered at higher magnification in panel B. Staining is representative of n=4 thrombi per group. **B,** Neutrophils are the predominant nucleated cells infiltrating thrombi at 6 hours. Representative examples are indicated with yellow arrowheads (although essentially all cells in this view represent neutrophils). **C,** Western blotting of total thrombus protein for citrullinated histone H3 (Cit-H3) and total histone H3 (H3). Quantification is in arbitrary units.

For quantification, N=6 per group (for APS: 3 from the APS 1 group and 3 from the APS 5 group). Mean and SEM are depicted. *p<0.05.

Figure 6 DNase administration and neutrophil depletion protect against APS IgG-accelerated thrombosis at 6 hours. Neutrophil depletion was with an anti-Ly6G monoclonal antibody, administered 24 hours before the first control/APS IgG injection. DNase was dosed only once, immediately following stenosis (all mice presented in this figure underwent the stenosis procedure). **A-C,** Thrombus weight for each of the 9 treatment groups at 6 hours. Each data point represents an individual mouse. Horizontal lines denote group means. **D,** Neutrophil depletion reduces the NET content of APS thrombi. Western blotting of total thrombus protein is for total histone H3 (H3) and citrullinated histone H3 (Cit-H3). Lanes were loaded with equal amounts of total protein. Mice treated with control IgG have low NET content at baseline (as in Figure 5C) and are not depicted here. **E,** The efficiency of neutrophil depletion did not differ between groups. The dashed line is the mean neutrophil count for the control-stenosis group of Figure 4A. **F**, The data of panels A-C is here presented as thrombosis frequency, and organized by treatment group. *p<0.05, **p<0.01, ns=not significant.

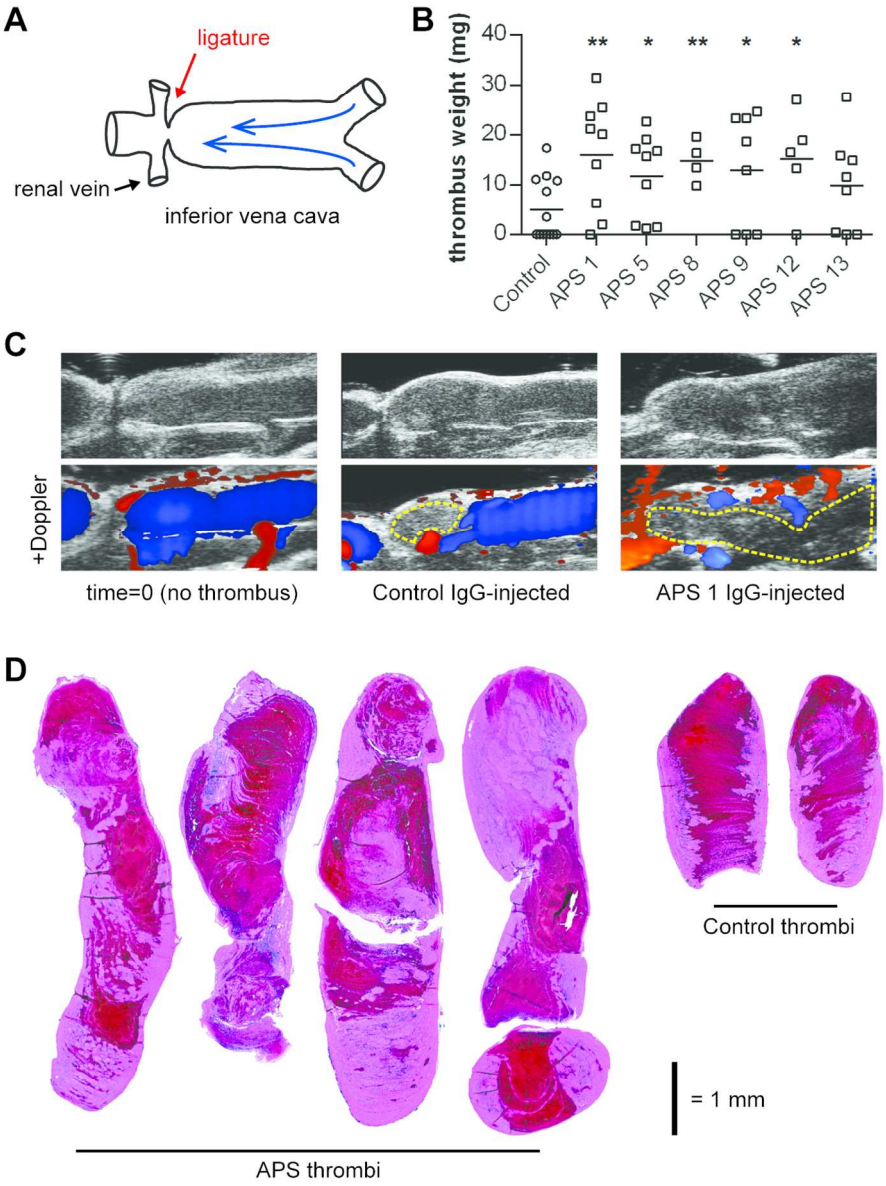

Figure 1

117x152mm (300 x 300 DPI)

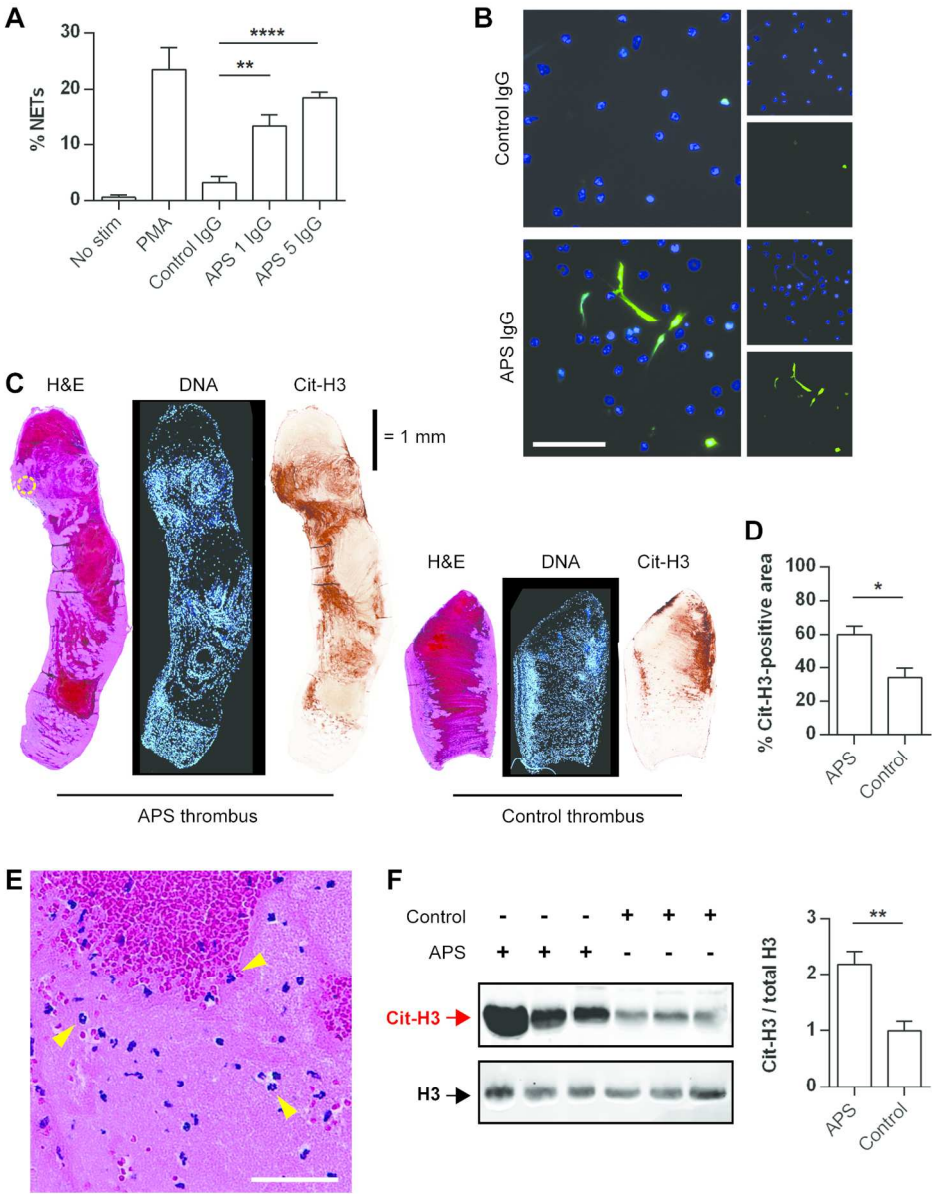

Figure 2

148x182mm (300 x 300 DPI)

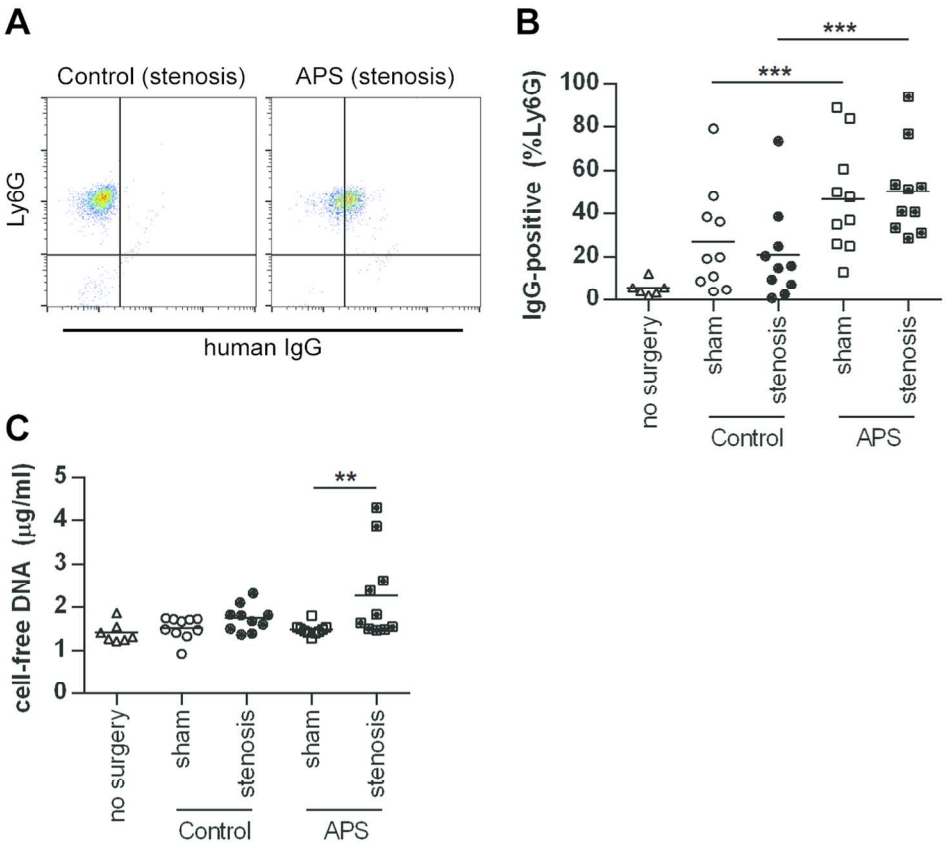

Figure 3

117x103mm (300 x 300 DPI)

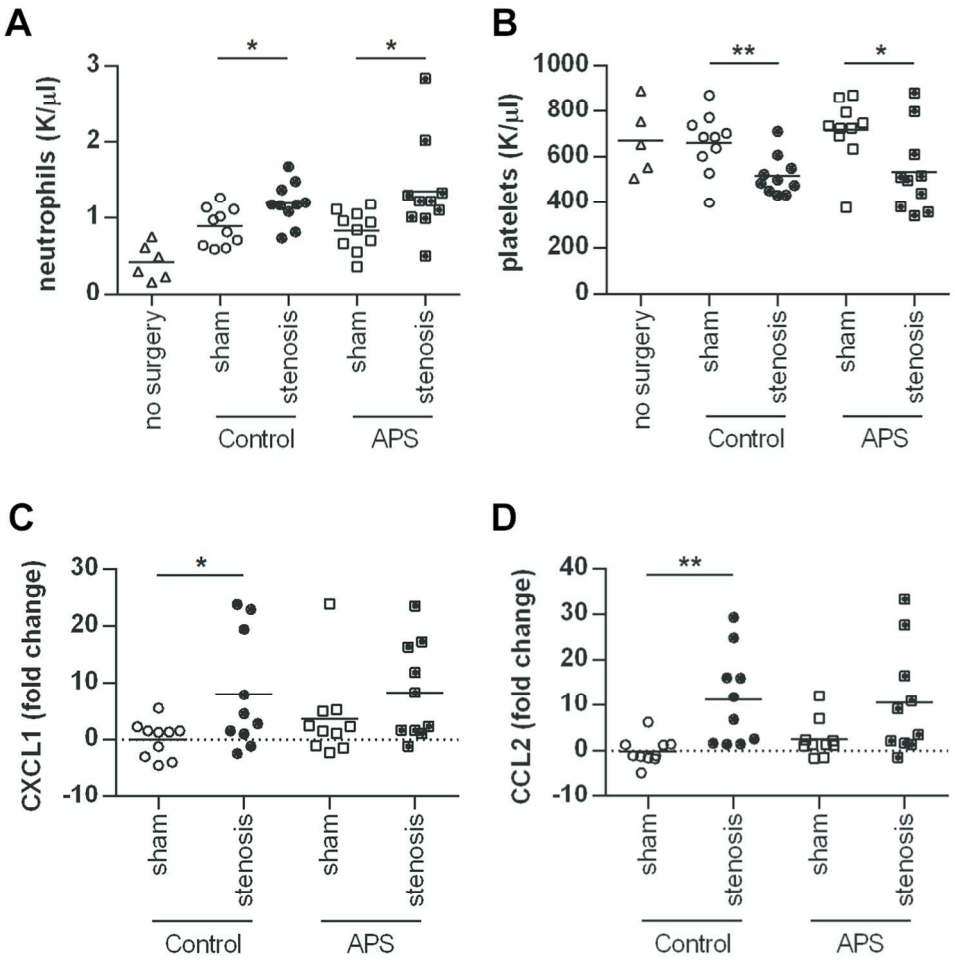

Figure 4

111x110mm (300 x 300 DPI)

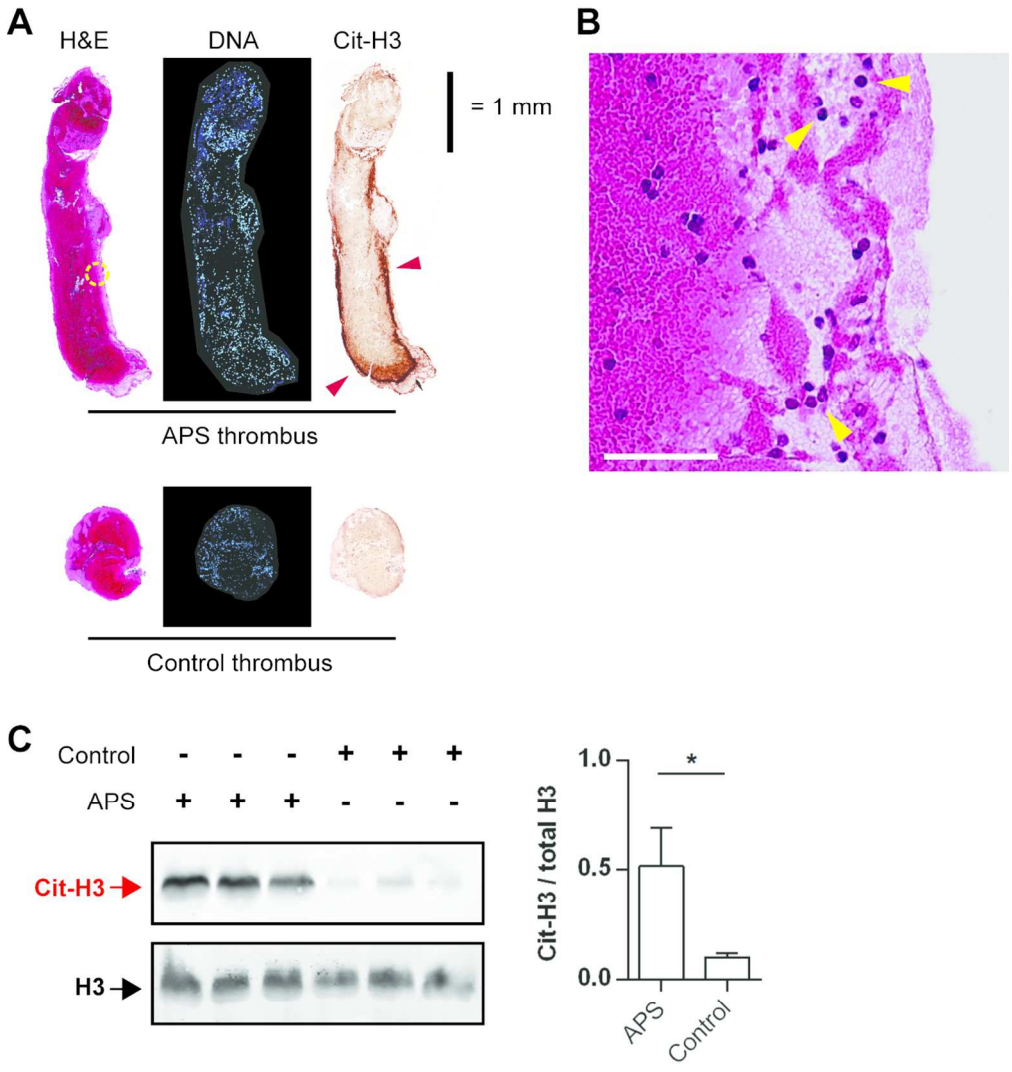

Figure 5

116x127mm (300 x 300 DPI)

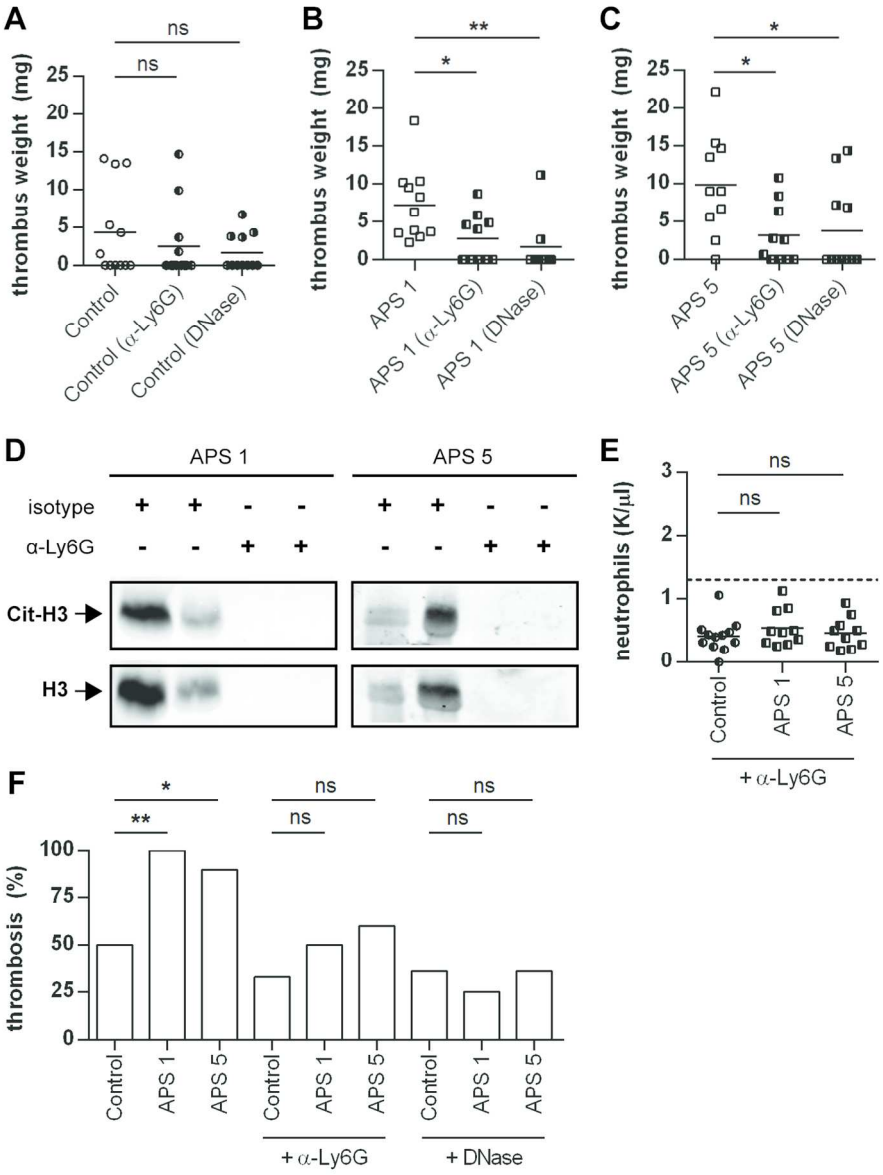

Figure 6

125x160mm (300 x 300 DPI)